Automatic 1D Convolutional Neural Network-based Detection of Artifacts in MEG acquired without Electrooculography or Electrocardiography

Prabhat Garg[1], Elizabeth Davenport[1], Gowtham Murugesan[1], Ben Wagner[1], Christopher Whitlow[2], Joseph Maldjian[1], Albert Montillo[1*]

[1]UT Southwestern Medical Center, Dallas, Texas, USA,
[2]Wake Forest School of Medicine, Winston-Salem, NC, USA
*Corresponding author: Albert.Montillo@UTSouthwestern.edu

***Abstract*— Magnetoencephalography (MEG) is a functional neuroimaging tool that records the magnetic fields induced by electrical neuronal activity; however, signal from non-neuronal sources can corrupt the data. Eye-Blinks (EB) and Cardiac Activity (CA) are two of the most common types of non-neuronal artifacts. They can be measured by affixing eye proximal electrodes, as in electrooculography (EOG) and chest electrodes, as in electrocardiography (EKG), however this complicates imaging setup, decreases patient comfort, and often induces further artifacts from facial twitching and postural muscle movement. We propose an EOG- and EKG-free approach to identify eye-blink, cardiac, or neuronal signals for automated artifact suppression.**

Our contributions are two-fold. First, we combine a data driven, multivariate decomposition approach based on Independent Component Analysis (ICA) and a highly accurate classifier constructed as a deep 1-D Convolutional Neural Network. Second, we visualize the features learned to reveal what features the model uses and to bolster user confidence in our model's training and potential for generalization. We train and test three variants of our method on resting state MEG data from 49 subjects. Our cardiac model achieves a 96% sensitivity and 99% specificity on the set-aside test-set. Our eye-blink model achieves a sensitivity of 85% and specificity of 97%. This work facilitates automated MEG processing for both, clinical and research use, and can obviate the need for EOG or EKG electrodes.

Keywords: MEG, artifact, EOG, EKG, deep learning, CNN.

I. Introduction

Magnetoencephalography (MEG), a functional neuroimaging method, offers better temporal resolution than fMRI [1, 2]. Compared to electroencephalography (EEG), MEG is less affected by intervening tissue characteristics, which results in a more accurate source space reconstruction [2–4]. Nevertheless, MEG is vulnerable to electromagnetic noise arising from non-neuronal sources. For example, the spectral bandwidth of muscle activity overlaps with the gamma-frequency band [4, 5]. Furthermore, eye-blink (EB) artifacts and cardiac artifacts (CA), which are two of the most common sources of artifact in MEG data, share frequency bands (1Hz – 20Hz) with alpha, theta, and delta waves [6, 7].

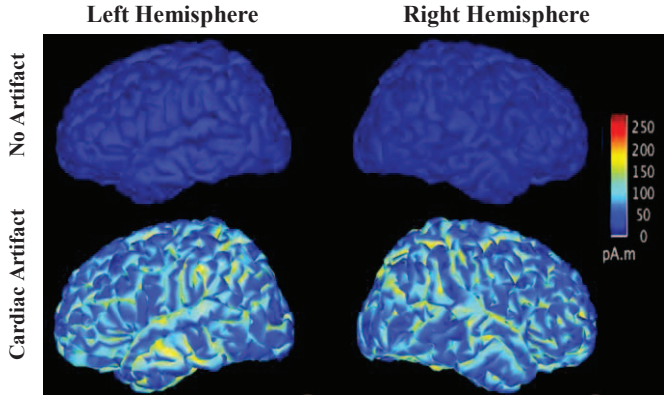

Fig. 1. Effect of cardiac artifacts on source space reconstruction of neuronal activity. A cardiac ICA component was manually identified and projected into brain space via MNE source localization. Top row: projection of signal between two heartbeats (without artifact). Bottom row: projection during a heartbeat. Diffuse activity is modeled across both hemispheres due to the artifact.

Fig. 1 shows how a CA can corrupt all areas of MEG brain source space reconstruction making its identification and suppression critical for mapping true brain activity.

Removing artifacts from MEG using Independent Component Analysis (ICA) improves MEG signal-to-noise ratio by 35%, while spectral approaches achieve an improvement of only 5-10% [8]. ICA decomposes the data into individual components, separating artifact and signal in the process. However, these components are randomly ordered and must be manually labeled as signal or artifact [4, 9]. To automate the process of detecting EB and CA artifacts, some researchers use electrooculography (EOG) and electrocardiography (ECG) electrodes to separately record the eye-blink and cardiac artifact signals [7]. However, these methods add complexity and time to the data acquisition setup, can be uncomfortable for the subjects, and can induce additional artifacts from postural muscle movements and/or facial twitching [4].

II. Methods

A. Data Collection and Preprocessing

8 minutes of resting state MEG data was obtained from 49 male football players: 19 high school (14-18 years old) and 30

youth (9-13 years), as part of the Imaging Telemetry And Kinematic modeling in youth football (iTAKL) concussion study [10]. To minimize ocular saccadic movement, subjects held their eyes open and fixated on a target. Data preprocessing included down-sampling to 250Hz, application of a notch filter to suppress to line noise, and band pass filtering to 1Hz-100Hz using Brainstorm [11].

B. Independent Component Analysis (ICA)

Using InfoMax ICA [12], the data was decomposed into 20 components. Each one of these components consists of a spatial map indicating areas of magnetic scalp influx and outflux and a time course (Fig 2) of the spatial map's activation. In this study, the time courses were the input feature utilized. The time courses from all 49 subjects were labeled by an expert rater with more than 5 years of experience in MEG image interpretation (ED)

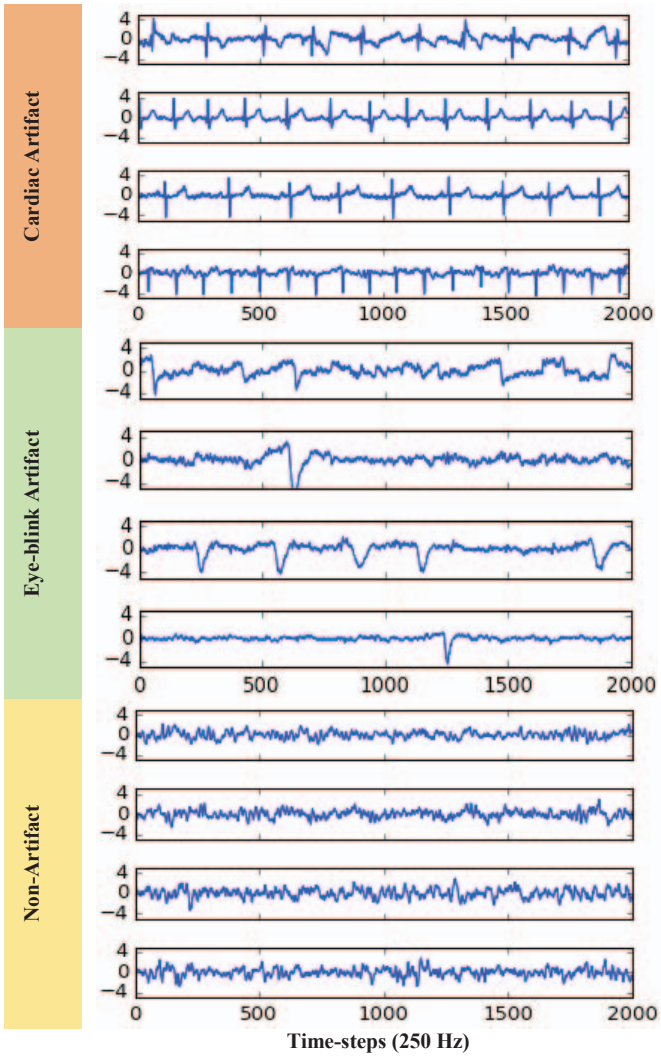

Fig. 2. Examples of time courses generated by ICA for each of the three signal categories of interest: cardiac, eye-blink, and non-artifact. The cardiac time course shows characteristic P-QRS-T complexes and regularity of an EKG, eye-blink time courses show broad signal dips that are less regular, while non-artifact signal show more broad spectrum (superposition of alpha, beta, delta wave signals).

C. Convolutional Neural Networks

Convolutional neural networks (CNN) have demonstrated remarkable success in the Image-net Large Scale Visual Recognition Challenge (ILSVRC) [13]. Such 2D-CNNs learn to recognize the local structure within an image. Inspired by these successes, the hypothesis for this study is that a 1D-CNN will be able to recognize local structure in our time courses signals. For example, a cardiac signal has peaks in a predictable order (Fig. 2, top third). Therefore, 1-D CNN based classifiers were constructed with the architecture shown in Fig. 3.

D. CNN Model development and testing

The model was trained using the 19 high school subjects. A leave-one-subject-out strategy was employed to optimize the hyper-parameters. The remaining 30 youth subjects were set aside for testing the model. These subjects were not used for optimizing any hyper-parameters. The separate dataset and age group was utilized for testing in order to provide a stronger assessment of the generalization capabilities of the model, as compared to testing on data from the same dataset.

Three different versions of the MEG-net were constructed. The first two are binary classifiers. Model 1 was trained to only detect cardiac artifact, while model 2 was trained to only detect the eye-blink artifact. Model 3, which is a 3-category classifier, was trained to detect both.

1) Input size

CNNs have a fixed input size that is decided prior to training, and we wanted to create classifiers that will generalize to data with recordings shorter than 8 minutes (120,000 time-steps). Thus, we trained classifiers that only require 40 seconds (10,000 time-steps) of input (Fig. 3, Right). Longer signals can be truncated and shorter signals can be extended to 40 seconds by repeating the existing signal.

2) Max-pooling

Because the shape of the individual P-QRS-T wave complex is variable among different subjects (Fig. 2, Cardiac), we suspect that a repeating *sequence* of multiple P-QRS-T complexes is more important than the morphology of an individual complex for accurately detecting a cardiac signal. The five pairs of convolution and max-pooling layers (Fig 3) allow us to create a receptive field in the last max-pooling layer that is large enough to recognize two consecutive complexes irrespective of the signal's phase. The last max-pooling layer is able to scan the input signal over 1.6 seconds. A subject who has one heartbeat every 1.6 seconds will have a heart rate of 37.5 beats/min. Any subject with higher heart rate than 37.5 beats/min will produce at least two complexes in our chosen receptive field. Since most people have heart rates between 60 beats/min to 100 beats/min, our model should be able to detect a cardiac signal regardless of the P-QRS-T complex morphology.

III. RESULTS

MEG-net-1 (cardiac only model) demonstrated remarkable accuracy (96% sensitivity and 99% specificity) for detecting the cardiac artifact. MEG-net-2 (eye-blink only model) also

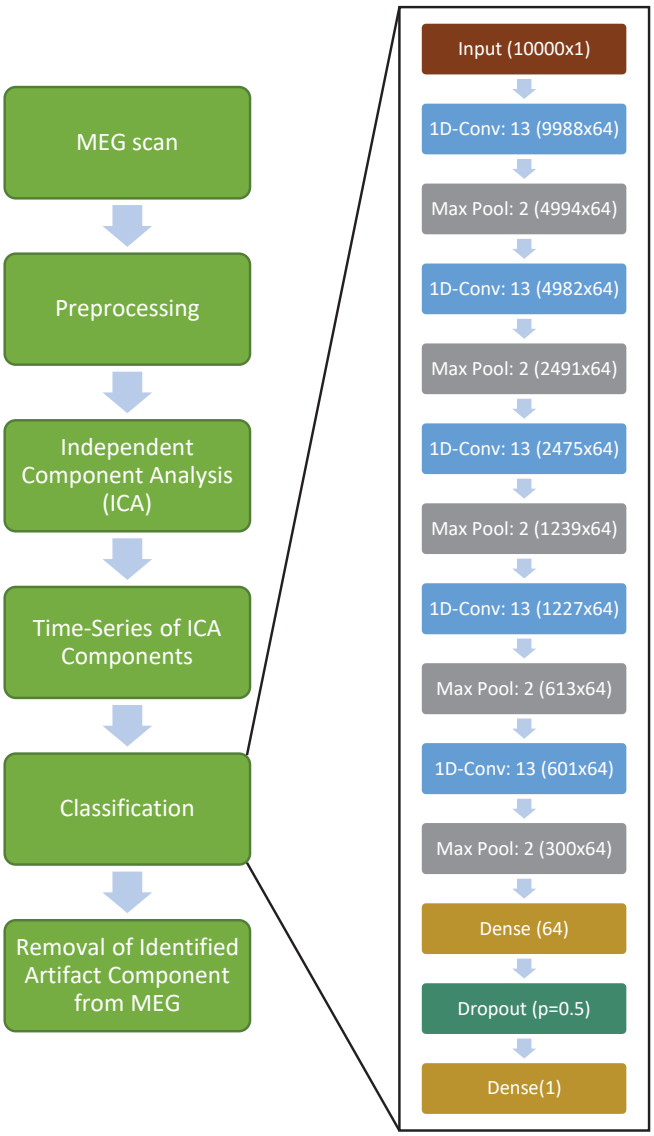

Fig. 3. Proposed processing pipeline. Left: Overall processing pipeline proceeds from resting state MEG acquisition, through preprocessing and automatic artifact identification and finally artifact suppression before reconstructing the brain signal without the artifact components. Right: CNN architecture includes several convolution and max pooling layers followed by fully connected or dense layers. For binary classification, the last layer has 1 neuron (shown), while for 3-category it has 3 one-hot-encoded neurons (not shown). The dropout layer allows for regularization by randomly setting some neurons in previous layers to zero during training. Our model requires only 10,000 time-points (40 seconds at 250Hz).

demonstrated promising results (85% sensitivity and 97% specificity). Full test results are summarized in Fig. 4 along with the respective confusion matrices for the held-out, test set which was not used during training or model selection.

IV. Discussion

A. Related Work

There is little existing research on the automation of MEG artifact removal without the use of supplementary electrodes (EOG, EKG). One exception is Duan et al. [1] in which a support vector machine (SVM) was trained with five manually selected features (Kurtosis, Probability Density, Central Moment of Frequency, Spectral Entropy, and Fractal Dimension) were extracted from the time series of ICA using data from 10 pediatric subjects. They report a cross-validation specificity of 99.65% and sensitivity of 92.01%. However, the small sample size used (10 subjects total) is a significant limitation of this study. In comparison, we train a 1-D convolutional neural network (CNN) using data from 19 subjects and report accuracy measures from a held-out set from a separate dataset and cohort containing 30 subjects. We also report *test* accuracy as opposed to *cross-validation* accuracy. Test accuracy tends to more accurately reflect real-world performance, while cross-validation accuracy tends to overestimate performance. Furthermore, our MEG-net uses the raw time series data and automatically learns the important features. Thus, we avoid manually selecting features that might add bias to our model.

B. Feature Visualization, Grad-CAM

In order to gain a deeper insight into what MEG-net has learned, gradient-weighted class activation maps (grad-CAM) [14] were generated to visualize learned features (Fig 5). MEG-net-3 was selected as an example because it can provide insight into how a model handles features for all three different classes. For illustrative purposes a time course was constructed that contains segments from all three classes as input for grad-CAM. The method provides information on three simple questions. 1) Which input features (time points) are most important for cardiac classification? 2) The eye-blink classification? 3) And, non-artifact classification? The time segments that are most important for artifact classifications correspond well with the time segments that human experts find discriminative for identifying the artifacts (Fig. 5). In particular, the peaks in the feature importance for eye-blink classification (Fig. 5, row 2, green curve) correspond appropriately to the eye-blink features shaded in green (Fig 5, row 1). Meanwhile, feature importance curves of cardiac and the non-artifact classes show little or no importance during these eye-blink time segments. Additionally, feature importance curve of non-artifact class (shown in yellow) displays highest importance in the non-artifact segment (row 1, right side). Lastly, the feature importance of cardiac class (red curve) has a high baseline and displays highest importance from the R and T waves in the cardiac segment (row 1, left).

V. Conclusion

We have proposed 1D-CNNs for the accurate detection of cardiac and eye-blink artifacts. The solution is fully automated and does not require current standard of care EOG or EKG recordings, which complicate imaging setup, decrease patient comfort, and often induce further artifacts. Additionally, using advanced visualizations, we demonstrate that the features our CNNs have learned correspond well with those used by human experts. Future work can extend the model to utilize spatial map data.

Acknowledgment

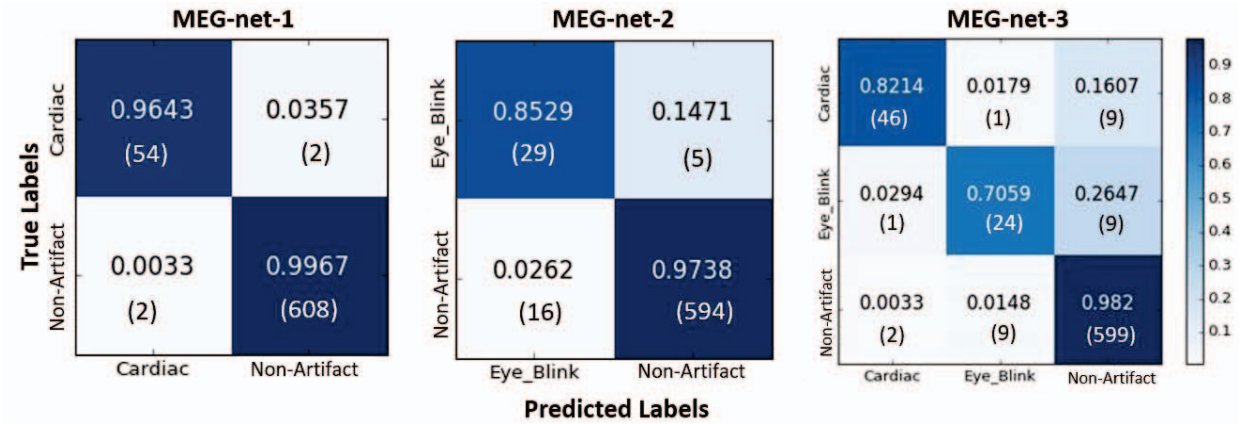

Fig. 4. Accuracy of our three MEG-net models shown as normalized confusion matrices. Left: CNN binary classifier that identifies cardiac artifacts. Center: CNN binary classifier, which identifies eye-blink artifacts. Right: Three-category CNN, which identifies cardiac, eye-blink and non-artifact components. Parentheses contain the numbers used to compute the normalized matrices.

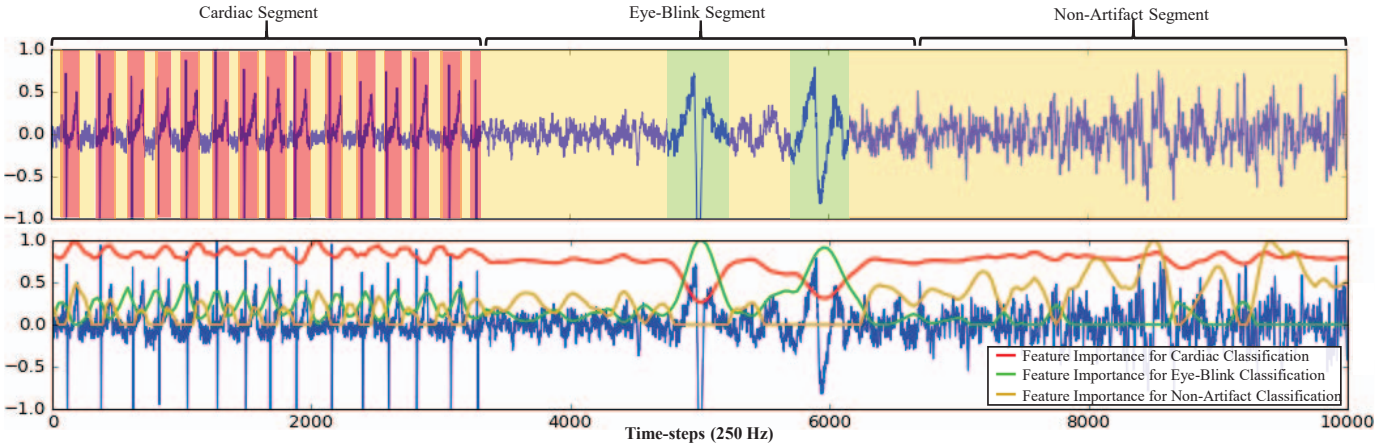

Fig. 5. Visualization of the features learned in MEG-net-3. Top row: Input consists of a time course with 3 segments: cardiac, eye-blink, and non-artifact signal (labeled on top of figure). With different colors, we shade the *features* human experts use to visually distinguish these three segments. Cardiac R and T waves are shaded red; eye-blinks are shaded green, while non-artifact features are shaded yellow. Bottom row: Gradient-weighted class activation maps (grad-CAM) are shown by the red, green and yellow curves. The red curve peaks for time points considered important for cardiac classification, green curve for those important for eye-blink classification, while yellow curve for those important for the non-artifact classification.

We thank Jillian Urban, Mireille Kelley, Derek Jones, and Joel Stitzel for assistance in recruitment and study oversight. Support for this research was provided by NIH grant R01NS082453 (JAM,JDS), R03NS088125 (JAM), and RO1NS091602 (CW,JAM,JDS).

REFERENCES

[1] F. Duan *et al.,* "Boosting specificity of MEG artifact removal by weighted support vector machine," *Conference proceedings: IEEE EMBS*, vol. 2013, pp. 6039–6042, 2013.

[2] Z. Fatima, M. A. Quraan, N. Kovacevic, and A. R. McIntosh, "ICA-based artifact correction improves spatial localization of adaptive spatial filters in MEG," *NeuroImage*, vol. 78, pp. 284–294, 2013.

[3] G. Buzsáki, C. a. Anastassiou, and C. Koch, "The origin of extracellular fields and currents - EEG, ECoG, LFP and spikes," *Nature reviews. Neuroscience*, vol. 13, no. 6, pp. 407–420, 2012.

[4] S. D. Muthukumaraswamy, "High-frequency brain activity and muscle artifacts in MEG/EEG: a review and recommendations," *Frontiers in Human Neuroscience*, vol. 7, no. April, p. 138, 2013.

[5] E. Criswell, *Cram's Introduction to Surface Electromyography*, 2011.

[6] T. Zikov, S. Bibian, G. A. Dumont, M. Huzmezan, and C. R. Ries, "A wavelet based de-noising technique for ocular artifact correction of the electroencephalogram," in *IEEE EMBS*, Oct. 2002, pp. 98–105.

[7] L. Breuer, J. Dammers, T. P. L. Roberts, and N. J. Shah, "Ocular and cardiac artifact rejection for real-time analysis in MEG," *Journal of Neuroscience Methods*, vol. 233, pp. 105–114, 2014.

[8] A. Gonzalez-Moreno *et al.,* "Signal-to-noise ratio of the MEG signal after preprocessing," *Journal of Neuroscience Methods*, vol. 222, pp. 56–61, 2014.

[9] J. Gross *et al.,* "Good practice for conducting and reporting MEG research," *NeuroImage*, vol. 65, pp. 349–363, 2013.

[10] E. M. Davenport *et al.,* "Abnormal white matter integrity related to head impact exposure in a season of high school varsity football," *Journal of neurotrauma*, vol. 31, no. 19, pp. 1617–1624, 2014.

[11] F. Tadel, S. Baillet, J. C. Mosher, D. Pantazis, and R. M. Leahy, "Brainstorm: a user-friendly application for MEG/EEG analysis," *Computational intelligence and neuroscience*, vol. 2011, p. 879716, 2011.

[12] A. J. Bell and T. J. Sejnowski, "An information-maximization approach to blind separation and blind deconvolution," *Neural computation*, vol. 7, no. 6, pp. 1129–1159, 1995.

[13] O. Russakovsky *et al.,* "ImageNet Large Scale Visual Recognition Challenge," *Int J Comput Vis*, vol. 115, no. 3, pp. 211–252, 2015.

[14] R. R. Selvaraju *et al.,* "Grad-CAM: Visual Explanations from Deep Networks via Gradient-based Localization," [Online] Available: https://arxiv.org/pdf/1610.02391.pdf. Accessed on: Apr. 04 2017.